2414 *Inorg. Chem.* **1989**, *28*, 2414–2419

Contribution from the Departments of Chemistry, Kansas State University, Manhattan, Kansas 66506,
and University of North Dakota, Grand Forks, North Dakota 58202

η^6-Arene Displacement by Halide Ions. Synthesis and Structural Characterization of Chloro- and Fluoro-Bridged Organonickel Complexes $[R_2MX]_2^{2-}$ ($R = C_6F_5$, $SiCl_3$; X = Halide)

Michael M. Brezinski,[†] Jeorg Schneider,[†] Lewis J. Radonovich,*[‡] and Kenneth J. Klabunde*[†]

Received September 14, 1988

A series of $[R_2MX]_2^{2-}$ halo-bridged complexes of Ni(II) have been prepared by halide substitution of arene in (η^6-arene)NiR_2 complexes. These are particularly unusual compounds, since no neutral donor ligands are present, and they are perhalogenated at the R group. The halo bridge was varied as F, Cl, and Br, and R was varied as C_6F_5 and $SiCl_3$. Several complexes were structurally characterized, which allowed assessments of the effect of X on Ni–C and Ni–Si bonds, bond angles, and other parameters, which helped to explain σ- and π-bonding abilities. Thus, the compound $[(\mu\text{-Cl})_2Ni_2(C_6F_5)_4][(C_2H_5)_4N]_2\cdot CH_2Cl_2$ crystallizes in space group $I\bar{1}$ with lattice constants of $a = 10.618$ (2) Å, $b = 13.652$ (3) Å, $c = 18.144$ (3) Å, $\alpha = 86.20$ (2)°, $\beta = 89.18$ (2)°, $\gamma = 93.02$ (2)°, and $Z = 2$. The compound $[(\mu\text{-Cl})_2Ni_2(SiCl_3)_4][((CH_3)_3C)_2C_5H_3NH]_2$ crystallizes in space group $P2_1/n$ with lattice constants of $a = 11.686$ (2) Å, $b = 11.683$ (2) Å, $c = 17.272$ (4) Å, $\beta = 87.645$ (6)°, and $Z = 2$. The compound $[(\mu\text{-F})_2Ni_2(C_6F_5)_4][(C_4H_9)_4N]_2$ crystallizes in space group *Pbca* with $a = 16.601$ (3) Å, $b = 21.717$ (5) Å, $c = 17.158$ (4) Å, and $Z = 4$. The three structures contain dimeric anions with a square-planar geometry that resides on crystallographic centers of inversion. Bond parameters in the dimer core are not changed significantly when C_6F_5 is replaced by $SiCl_3$, but relatively large changes are observed when the bridging chloride is replaced by fluoride.

Introduction

Investigations of coordinatively unsaturated organonickel, -palladium, -platinum, and -cobalt species such as RMX and R_2M have led to some unexpected results.[1-5] Unusually high thermal stabilities but high chemical reactivities are trademarks of RMX and R_2M species where R = C_6F_5, C_6Cl_5, SiF_3, or $SiCl_3$. Another expectation is their ability to bind a variety of weak ligands including ethers, thioethers, amines, and arenes. Similarly, due to the high lability of the η^6-arene ligand, the complexes (η^6-arene)NiR_2 and (η^6-arene)CoR_2 have proven to be very useful in catalysis and other chemical processes.[6]

From the list above it is clear that these RMX and R_2M species are electronically stabilized by the presence of highly electronegative substituents on the R groups, and structural data suggests that some π-back-bonding is involved. It is interesting to compare the R groups to halides (X) and note that the RMX and R_2M species have much greater solubilities and greater tendencies to ligate than MX_2. An assumption has been that the RMX species could help stabilize itself in the absence of donor ligands, by halide bridging.[1] However, no structural data supporting this has been available. With this idea in mind, and with our experience with π-arene displacements,[7] we attempted to prepare halide-bridged R_2M species:

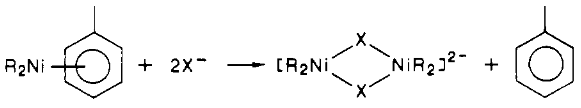

Although halo-bridging in group 8–10 metal complexes is certainly not new,[8-14] such complexes with σ-bound R groups are somewhat rare, and those with only σ-R groups (no neutral ligands) are very unusual. Uson and co-workers have prepared the closest analogues:[15-18]

$$\mathrm{Cl_2PdL_2 + BrTl(C_6F_5)_2 \rightarrow \tfrac{1}{2}(C_6F_5)LPd(\mu\text{-}Cl)_2PdL(C_6F_5) + TlBr + C_6F_5Cl + L}$$

We now report the synthesis of a new series of unusual $(R_2MX)_2$ halo-bridged compounds along with spectral and structural data. Compounds prepared are shown below (**1**–**6**). They are particularly unusual because no neutral donor ligands are present, and they are all perhalogenated.

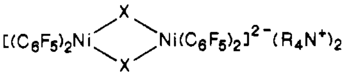

X = F, R = *n*-Bu (**1**); X = Cl, R = Et (**2**)

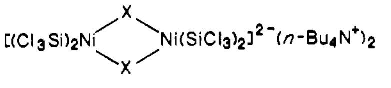

X = F (**3**), Cl (**4**), Br (**5**)

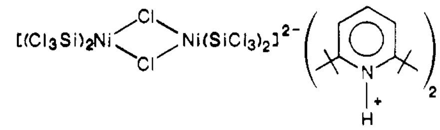

6

Results and Discussion

A. Preparative Routes. In all cases desired, known (η^6-arene)NiR_2 derivatives were prepared by either metal-vapor routes or organometallic synthetic pathways reported earlier.[2,4,19,20] Once the pure arene complex was obtained, products **1**–**5** were produced by treatment of the arene complex with tetraalkylammonium halide salts in organic solvents. Arene displacements took place

---

[†] Kansas State University.

[‡] University of North Dakota.

(1) Klabunde, K. J.; Anderson, B. B.; Neuenschwander, K. *Inorg. Chem.* **1980**, *19*, 3719–3724.
(2) Lin, S. T.; Narske, R. N.; Klabunde, K. J. *Organometallics* **1985**, *3*, 571–574.
(3) Brezinski, M.; Klabunde, K. J. *Organometallics* **1983**, *2*, 1116.
(4) Groshens, T. J.; Klabunde, K. J. *Organometallics* **1982**, *1*, 564.
(5) Groshens, T. J.; Klabunde, K. J. *J. Organomet. Chem.* **1983**, *259*, 337–343.
(6) Kanai, H.; Choe, S. B.; Klabunde, K. J. *J. Am. Chem. Soc.* **1986**, *108*, 2019–2023.
(7) Brezinski, M.; Klabunde, K. J.; Janakowski, S. K.; Radonovich, L. J. *Inorg. Chem.* **1985**, *24*, 3305–3307.
(8) Hartley, F. R. *Organomet. Chem. Rev., Sect. A* **1970**, *6*, 119.
(9) Eaborn, C.; Odell, K. J.; Pidcock, A. *J. Chem. Soc., Dalton Trans.* **1978**, 1288.
(10) Nyholm, R. S.; Royo, P. *J. Chem. Soc., Chem. Commun.* **1969**, 421.
(11) Mason, R.; Textor, M. *J. Chem. Soc., Chem. Commun.* **1976**, 292–293.
(12) Anderson, G. K.; Cross, R. J. Manojlovic-Muir, L.; Muir, K. W.; Solomon, T. *J. Organomet. Chem.* **1979**, *170*, 385–397.
(13) Anderson, G. K. *Organometallics* **1983**, *2*, 665.
(14) Parra-Hake, M.; Rettig, M. F.; Wing, R. M.; Woolcock, J. C.; *Organometallics* **1982**, *1*, 1478–1480.
(15) Uson, R.; Fornies, J.; Martinez, F. *J. Organomet. Chem.* **1975**, *90*, 367; **1977**, *132*, 429.
(16) Uson, R.; Fornies, J.; Navarro, R. *Inorg. Chim. Acta* **1979**, *33*, 69–75.
(17) Uson, R.; Fornies, J.; Martinez, F.; Tonias, M.; Reoyo, I. *Organometallics* **1983**, *2*, 1386.
(18) Uson, R.; Fornies, J.; Martinez, F.; Tomas, M. *J. Chem. Soc., Dalton Trans.* **1980**, 888.
(19) Choe, S. B.; Klabunde, K. J. *Organomet. Synth.* **1986**, *3*, 153–155.
(20) Lin, S. T.; Klabunde, K. J. *Organomet. Synth.* **1986**, *3*, 147–149.

0020-1669/89/1328-2414$01.50/0 © 1989 American Chemical Society

Table I. Atomic Coordinates in $[(\mu\text{-Cl})_2Ni_2(C_6F_5)_4][Et_4N]_2 \cdot CH_2Cl_2$ (**2**)

atom	*x*	*y*	*z*	*B*,[a] Å^2
Ni	0.47792 (4)	0.4670 (3)	0.41195 (2)	5.31
Cl	0.45709 (7)	0.60653 (5)	0.48993 (3)	6.15
C(1a)	0.4894 (3)	0.3844 (2)	0.3482 (2)	6.13
C(2a)	0.4045 (3)	0.3036 (2)	0.3517 (2)	6.60
C(3a)	0.4073 (5)	0.2290 (3)	0.3062 (2)	8.44
C(4a)	0.4996 (6)	0.2296 (4)	0.2552 (2)	9.16
C(5a)	0.5857 (5)	0.3055 (4)	0.2474 (2)	9.17
C(6a)	0.5809 (4)	0.3789 (3)	0.2941 (2)	7.25
F(2a)	0.3073 (2)	0.2980 (2)	0.4032 (1)	8.34
F(3a)	0.3166 (4)	0.1522 (2)	0.3136 (2)	11.07
F(4a)	0.5058 (5	0.1531 (3)	0.2097 (2)	13.84
F(5a)	0.6791 (4)	0.3049 (4)	0.1954 (2)	13.28
F(6a)	0.6705 (2)	0.4533 (2)	0.2854 (1)	9.92
C(1b)	0.4267 (3)	0.5662 (2)	0.3304 (1)	5.82
C(2b)	0.3140 (3)	0.5532 (2)	0.2961 (2)	6.32
C(3b)	0.2762 (4)	0.6093 (3)	0.2365 (2)	7.40
C(4b)	0.3550 (6)	0.6835 (4)	0.2072 (2)	8.92
C(5b)	0.4657 (6)	0.7015 (3)	0.2377 (2)	9.02
C(6b)	0.5022 (4)	0.6445 (3)	0.2986 (2)	7.50
F(2b)	0.2290 (2)	0.4787 (2)	0.3225 (1)	7.53
F(3b)	0.1608 (3)	0.5914 (2)	0.2065 (1)	10.63
F(4b)	0.3179 (4)	0.7397 (2)	0.1461 (1)	12.60
F(5b)	0.5464 (5)	0.7777 (3)	0.2103 (2)	13.37
F(6b)	0.6159 (2)	0.6650 (2)	0.3254 (2)	10.06
N(1c)	0.000000	0.500000	0.500000	5.52
C(1c)	0.0972 (6)	0.5814 (4)	0.4712 (3)	7.35
C(2c)	0.103 (1)	0.6666 (6)	0.5228 (7)	8.68
C(3c)	−0.1279 (5)	0.5443 (6)	0.5142 (4)	7.82
C(4c)	−0.172 (2)	0.604 (2)	0.4452 (8)	12.44
C(5c)	0.0421 (6)	0.4529 (7)	0.5743 (3)	9.40
C(6c)	0.1748 (7)	0.414 (1)	0.5673 (7)	8.45
C(7c)	−0.0131 (6)	0.4225 (4)	0.4431 (3)	7.60
C(8c)	−0.132 (1)	0.3541 (8)	0.4571 (7)	8.77
N(1d)	0.500000	0.000000	0.500000	6.88
C(1d)	0.6339 (5)	0.0289 (5)	0.5250 (5)	9.46
C(2d)	0.678 (2)	0.1334 (9)	0.495 (1)	12.94
C(3d)	0.5034 (9)	−0.0195 (9)	0.4178 (3)	12.05
C(4d)	0.609 (1)	−0.086 (1)	0.3974 (8)	12.64
C(5d)	0.4130 (6)	0.0843 (5)	0.5115 (4)	8.87
C(6d)	0.428 (1)	0.124 (1)	0.5885 (5)	9.85
C(7d)	0.452 (1)	−0.0934 (5)	0.5455 (6)	12.96
C(8d)	0.312 (2)	−0.117 (2)	0.531 (2)	17.11
X(1)	0.969 (1)	−0.0505 (8)	0.4667 (6)	8.63
X(2)	0.962 (2)	−0.049 (2)	0.569 (2)	13.99
X(3)	0.934 (1)	−0.090 (1)	0.5130 (8)	10.21
X(4)	0.998 (1)	−0.008 (1)	0.3936 (9)	11.82
X(5)	0.945 (2)	−0.060 (2)	0.617 (2)	10.67
X(6)	0.979 (1)	−0.0246 (9)	0.5279 (8)	6.35
X(7)	0.936 (2)	−0.077 (2)	0.421 (1)	10.37
X(8)	0.916 (2)	−0.116 (2)	0.467 (2)	11.34
X(9)	0.919 (2)	−0.120 (1)	0.5775 (9)	9.46

[a] The thermal parameters are of the form $B = 8\pi^2 U^{-2}$.

smoothly. The products were then recovered by the sequence filtration, solvent removal, and recrystallization. Compound **6** was obtained by a more indirect route. When (η^6-arene)$Ni(SiCl_3)_2$ was treated with wet di-*tert*-butylpyridine, **6** was formed, and a plausible sequence for this reaction involving a proton transfer is given as

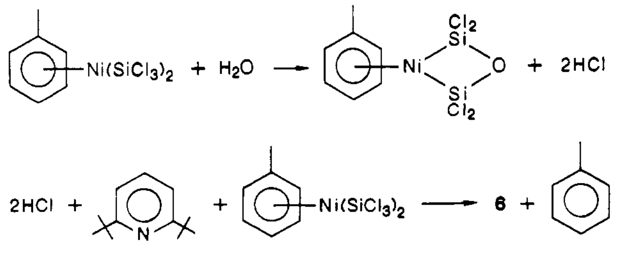

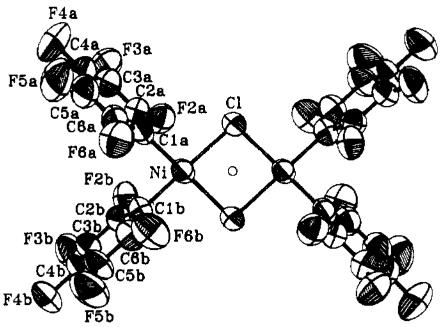

Figure 1. Computer drawing of the $[\mu\text{-Cl})_2Ni_2(C_6F_5)_4{}^{2-}$ anion as it exists in crystals of the $[Et_4N^+]_2$ salt. The circle indicates a crystallographic center of inversion.

Table II. Bond Distances (Å) in $[(\mu\text{-Cl})_2Ni_2(C_6F_5)_4][Et_4N]_2 \cdot CH_2Cl_2$ (**2**)

Ni–Cl	2.249 (1)	C(4b)–C(5b)	1.325 (8)
Ni–Cl′	2.257 (1)	C(4b)–F(4b)	1.379 (5)
Ni–C(1a)	1.880 (3)	C(5b)–C(6b)	1.380 (6)
Ni–C(1b)	1.880 (3)	C(5b)–F(5b)	1.374 (6)
C(1a)–C(2a)	1.385 (4)	C(6b)–F(6b)	1.331 (5)
C(1a)–C(6a)	1.379 (5)	N(1c)–C(1c)	1.536 (5)
C(2a)–C(3a)	1.354 (5)	N(1c)–C(3c)	1.541 (6)
C(2a)–F(2a)	1.378 (4)	N(1c)–C(5c)	1.537 (5)
C(3a)–C(4a)	1.338 (7)	N(1c)–C(7c)	1.529 (6)
C(3a)–F(3a)	1.385 (5)	C(1c)–C(2c)	1.54 (1)
C(4a)–C(5a)	1.343 (8)	C(3c)–C(4c)	1.53 (2)
C(4a)–F(4a)	1.377 (6)	C(5c)–C(6c)	1.53 (1)
C(5a)–C(6a)	1.357 (6)	C(7c)–C(8c)	1.53 (1)
C(5a)–F(5a)	1.360 (6)	N(1d)–C(1d)	1.538 (6)
C(6a)–F(6a)	1.354 (4)	N(1d)–C(3d)	1.533 (6)
C(1b)–C(2b)	1.364 (4)	N(1d)–C(5d)	1.536 (7)
C(1b)–C(6b)	1.391 (4)	N(1d)–C(7d)	1.532 (8)
C(2b)–C(3b)	1.362 (5)	C(1d)–C(2d)	1.54 (2)
C(2b)–F(2b)	1.380 (3)	C(3d)–C(4d)	1.53 (2)
C(3b)–C(4b)	1.355 (6)	C(5d)–C(6d)	1.53 (1)
C(3b)–F(3b)	1.364 (5)	C(7d)–C(8d)	1.53 (2)
Ni–Ni	3.277 (1)	Cl–Cl	3.094 (1)

B. Structural Comparisons. Since the nature of the R group is so critical in stabilizing these types of compounds, the availability of compounds **1**–**6** as crystalline solids provides the opportunity for quantitative structural comparisons. First, the structure of $[(C_6F_5)_2Ni(\mu\text{-Cl})_2Ni(C_6F_5)_2]^{2-}$ (**2**) will be compared to the structure of $[(Cl_3Si)_2Ni(\mu\text{-Cl})_2Ni(SiCl_3)_2]^{2-}$ (**6**) with particular emphasis on the Ni_2Cl_2 core.

The anion of **2** contains two nickel atoms with each nickel atom σ-bonded to two C_6F_5 groups and two chloride ligands. The chloride ligands function as bridges between the two nickel atoms. A computer drawing of this dianion is shown in Figure 1 along with the atomic numbering scheme for the asymmetric unit of structure. The atomic coordinates are listed in Table I, and the associated bond distances and angles are listed in Tables II and III, respectively. The geometry of the dimeric $NiCl_2$ Ni moiety is rigorously square planar (0° fold angle) with the halves of the dimer related by a crystallographic center of inversion. The local geometry within each nickel coordination sphere is approximately square planar. The average deviation of the five atoms (Ni, Cl, Cl′, C(1a), C(1b)) from planarity is 0.024 Å. This small deviation expressed as a rotation angle between planes defined by Ni, Cl, Cl′ and Ni, C(1a), C(1b) is 2.4°. The C_6F_5 groups are canted approximately 18° from the normal to the coordination plane. The CNiC angle is 87.6 (1)°. The Ni–C_6F_5 bond length of 1.880 (3) Å is the same as that reported for $(C_6F_5)BrNi[PCH_3(C_6H_5)_2]_2$,[21] which also has a C_6F_5 group trans to a halogen. The C_6F_5 groups have typical bond parameters,[22,23] with an internal ring angle at the metal-bound carbon of 112.0 (3)°.

The crystal structure of **6** is similar to that of **2**. The unit cell of **6** contains four $[((CH_3)_3C)_2C_5H_3NH]^+$ cations and two dimeric anions of composition $[(Cl_3Si)_2Ni(\mu\text{-Cl})_2Ni(SiCl_3)_2]^{2-}$. The two

---

(21) Churchill, M. R.; Kalra, K. L.; Veidis, M. V. *Inorg. Chem.* **1973**, *12*, 1656.

(22) Churchill, M. R.; Veidis, M. V. *J. Chem. Soc. A* **1971**, 3464.

(23) Eyring, M. W.; Radonovich, L. J. *Organometallics* **1985**, *4*, 1841 and references therein.

Table III. Bond Angles (deg) in $[(\mu\text{-Cl})_2Ni_2(C_6F_5)_4][Et_4N]_2\cdot CH_2Cl_2$ (**2**)

Cl–Ni–Cl′	86.71 (3)	C(1b)–C(2b)–C(3b)	124.95 (30)
Cl–Ni–C(1a)	177.80 (9)	C(1b)–C(2b)–F(2b)	119.49 (25)
Cl–Ni–C(1b)	92.82 (9)	C(3b)–C(2b)–F(2b)	115.56 (29)
Cl′–Ni–C(1a)	92.88 (9)	C(2b)–C(3b)–C(4b)	118.95 (38)
Cl′–Ni–C(1b)	178.86 (9)	C(2b)–C(3b)–F(3b)	120.77 (32)
C(1a)–Ni–C(1b)	87.63 (13)	C(4b)–C(3b)–F(3b)	120.28 (35)
Ni–Cl–Ni′	93.29 (3)	C(3b)–C(4b)–C(5b)	119.74 (38)
Ni–C(1a)–C(2a)	122.33 (23)	C(3b)–C(4b)–F(4b)	119.24 (47)
Ni–C(1a)–C(6a)	125.62 (25)	C(5b)–C(4b)–F(4b)	121.02 (44)
C(2a)–C(1a)–C(6a)	112.04 (29)	C(4b)–C(5b)–C(6b)	120.58 (42)
C(1a)–C(2a)–C(3a)	124.57 (33)	C(4b)–C(5b)–F(5b)	121.08 (41)
C(1a)–C(2a)–F(2a)	119.15 (27)	C(6b)–C(5b)–F(5b)	118.34 (47)
C(3a)–C(2a)–F(2a)	116.25 (32)	C(1b)–C(6b)–C(5b)	122.44 (37)
C(2a)–C(3a)–C(4a)	119.36 (42)	C(1b)–C(6b)–F(6b)	120.04 (30)
C(2a)–C(3a)–F(3a)	120.08 (39)	C(5b)–C(6b)–F(6b)	117.49 (36)
C(4a)–C(3a)–F(3a)	120.55 (40)	C(1c)–N(1c)–C(3c)	109.90 (34)
C(3a)–C(4a)–C(5a)	120.13 (47)	C(1c)–N(1c)–C(5c)	110.06 (33)
C(3a)–C(4a)–F(4a)	120.14 (48)	C(1c)–N(1c)–C(7c)	109.05 (30)
C(5a)–C(4a)–F(4a)	119.72 (47)	C(3c)–N(1c)–C(5c)	106.95 (33)
C(4a)–C(5a)–C(6a)	119.14 (43)	C(3c)–N(1c)–C(7c)	110.60 (36)
C(4a)–C(5a)–F(5a)	119.44 (49)	C(5c)–N(1c)–C(7c)	110.26 (38)
C(6a)–C(5a)–F(5a)	121.35 (47)	N(1c)–C(1c)–C(2c)	110.83 (54)
C(1a)–C(6a)–C(5a)	124.66 (37)	N(1c)–C(3c)–C(4c)	111.35 (77)
C(1a)–C(6a)–F(6a)	117.83 (31)	N(1c)–C(5c)–C(6c)	110.88 (54)
C(5a)–C(6a)–F(6a)	117.49 (35)	N(1c)–C(7c)–C(8c)	112.15 (58)
Ni–C(1b)–C(2b)	124.24 (21)	C(1d)–N(1d)–C(3d)	109.56 (45)
Ni–C(1b)–C(6d)	122.43 (23)	C(1d)–N(1d)–C(5d)	109.65 (37)
C(2b)–C(1b)–C(6b)	113.33 (27)	C(1d)–N(1d)–C(7d)	108.63 (49)
C(3d)–N(1c)–C(5d)	108.91 (50)	C(1d)–C(3d)–C(4d)	113.01 (77)
C(3d)–N(1c)–C(7d)	109.71 (57)	N(1d)–C(5d)–C(6d)	111.61 (67)
C(5d)–N(1d)–C(7d)	110.37 (46)	N(1d)–C(7d)–C(8d)	110.8 (1.3)
N(1d)–C(1c)–C(2d)	111.87 (79)		

Table IV. Atomic Coordinates in $[(\mu\text{-Cl})_2Ni_2(SiCl_3)_4][((CH_3)_3C)_2C_5H_3NH]_2$ (**6**)

	x	*y*	*z*
Ni	0.0803 (1)	0.0989 (1)	0.0379 (1)
C(01)	−0.4219 (8)	0.1971 (10)	0.1908 (6)
C(03)	−0.4105 (10)	0.3985 (11)	0.1756 (8)
C(04)	−0.3626 (10)	0.3879 (10)	0.1006 (8)
C(05)	−0.3430 (8)	0.2805 (9)	0.0681 (6)
C(06)	−0.4456 (9)	0.0843 (10)	0.2293 (6)
C(07)	−0.5237 (11)	0.1058 (13)	0.3008 (7)
C(08)	−0.5060 (10)	0.0015 (10)	0.1758 (7)
C(09)	−0.3328 (10)	0.0329 (10)	0.2554 (7)
C(10)	−0.2934 (10)	0.2559 (10)	−0.0116 (6)
C(11)	−0.3506 (12)	0.3332 (14)	−0.0710 (7)
C(12)	−0.1624 (9)	0.2832 (12)	−0.0084 (7)
C(13)	−0.3088 (12)	0.1262 (11)	−0.0329 (7)
N(01)	−0.3727 (6)	0.1928 (7)	0.1166 (5)
Cl(1)	−0.0498 (3)	−0.0312 (3)	0.0811 (1)
Cl(2)	0.2561 (3)	0.2140 (3)	−0.1176 (2)
Cl(3)	0.1513 (3)	0.3917 (3)	0.0069 (2)
Cl(4)	0.3651 (3)	0.2230 (4)	0.0449 (2)
Cl(5)	0.1555 (3)	0.0213 (3)	0.2230 (2)
Cl(6)	−0.0619 (2)	0.1963 (3)	0.2072 (2)
Cl(7)	0.1933 (3)	0.2891 (3)	0.1979 (2)
Si(1)	0.2059 (2)	0.2244 (2)	−0.0008 (2)
Si(2)	0.0971 (2)	0.1560 (2)	0.1571 (2)
H(02A)	−0.4742	0.3171	0.2722
H(03A)	−0.4243	0.4788	0.1987
H(04A)	−0.3421	0.4599	0.0686
H(01A)	−0.3569	0.1127	0.0954

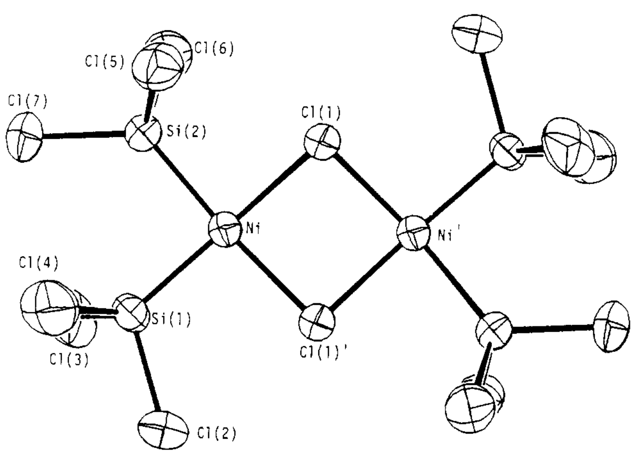

Figure 2. The $[(SiCl_3)_2NiClClNi(SiCl_3)_2]^{2-}$ anion. Prime notation is used to indicate those atoms related by a crystallographic center of inversion.

Table V. Bond Distances (Å) in $[(\mu\text{-Cl}_2)Ni_2(SiCl_3)_4][((CH_3)_3C)_2C_5H_3NH]_2$ (**6**)

Ni–Si(1)	2.161 (3)	C(06)–C(07)	1.526 (14)
Ni-Si(2)	2.181 (3)	C(06)–C(08)	1.530 (15)
Ni–Cl(1)	2.244 (3)	C(06)–C(09)	1.533 (15)
Ni–Cl(1)	2.255 (3)	C(10)–C(11)	1.540 (16)
C(01)–C(02)	1.362 (14)	C(10)–C(12)	1.567 (15)
C(01)–N(01)	1.384 (11)	C(10)–C(13)	1.571 (15)
C(01)–C(06)	1.497 (14)	Cl(2)–Si(1)	2.081 (4)
C(02)–C(03)	1.343 (15)	Cl(3)–Si(1)	2.059 (4)
C(03)–C(04)	1.395 (16)	Cl(4)–Si(1)	2.051 (4)
C(04)–C(05)	1.390 (14)	Cl(5)–Si(2)	2.074 (4)
C(05)–N(01)	1.359 (12)	Cl(6)–Si(2)	2.071 (4)
C(05)–C(10)	1.499 (14)	Cl(7)–Si(2)	2.060 (4)

Table VI. Bond Angles (deg) in $[(\mu\text{-Cl})_2Ni_2(SiCl_3)_4][((CH_3)_3C)_2C_5H_3NH]_2$ (**6**)

Si(1)–Ni–Si(2)	89.89 (11)	C(05)–C(10)–C(11)	109.71 (95)
Si(1)–Ni–Cl(1)	95.00 (11)	C(05)–C(10)–C(12)	105.66 (93)
Si(1)–Ni–Cl(1)	178.69 (12)	C(05)–C(10)–C(13)	110.86 (90)
Si(2)–Ni–Cl(1)	175.03 (12)	C(11)–C(10)–C(12)	100.83 (1.0)
Si(2)–Ni–Cl(1)	88.82 (11)	C(11)–C(10)–C(13)	110.64 (1.1)
Cl(1)–Ni–Cl(1)	86.29 (10)	C(12)–C(10)–C(13)	109.03 (1.0)
C(02)–C(01)–N(01)	113.62 (98)	C(05)–N(01)–C(01)	128.99 (87)
C(02)–C(01)–C(06)	130.15 (94)	Ni–Cl(1)–Ni′	93.71 (10)
N(01)–C(01)–C(06)	116.21 (89)	Cl(4)–Si(1)–Cl(3)	105.45 (20)
C(03)–C(02)–C(01)	122.47 (99)	Cl(4)–Si(1)–Cl(2)	98.55 (17)
C(02)–C(03)–C(04)	120.89 (1.1)	Cl(4)–Si(1)–Ni	119.40 (17)
C(05)–C(04)–C(03)	120.55 (1.1)	Cl(3)–Si(1)–Cl(2)	101.09 (19)
N(01)–C(05)–C(04)	113.45 (95)	Cl(3)–Si(1)–Ni	114.80 (16)
N(01)–C(05)–C(10)	120.04 (93)	Cl(2)–Si(1)–Ni	114.90 (16)
C(04)–C(05)–C(10)	126.51 (1.0)	Cl(7)–Si(2)–Cl(6)	100.27 (17)
C(01)–C(06)–C(07)	107.95 (99)	Cl(7)–Si(2)–Cl(5)	100.87 (18)
C(01)–C(06)–C(08)	111.70 (88)	Cl(7)–Si(2)–Ni	128.72 (16)
C(01)–C(06)–C(09)	109.26 (89)	Cl(6)–Si(2)–Cl(5)	104.65 (17)
C(07)–C(06)–C(08)	108.51 (96)	Cl(6)–Si(2)–Ni	110.48 (16)
C(07)–C(06)–C(09)	108.63 (93)	Cl(5)–Si(2)–Ni	109.30 (16)
C(08)–C(06)–C(09)	110.70 (99)		

Table VII. Comparison of Selected Bond Parameters[a] for the $[NiX_2R_2]_2^{2-}$ Ion in **1**, **2**, and **6**

compd	Ni–X, Å	X–Ni–X, deg	Ni---Ni, Å	X---X, deg	dihedral angle,[b] deg	Ni–R, Å
2	2.253 (1)	86.71 (3)	3.28	3.09	2.4	1.880 (3)
6	2.250 (3)	86.3 (1)	3.28	3.08	0.9	2.171 (3)
1	1.903 (2)	81.41 (7)	2.88	2.48	2.2	1.906 (3)

[a] X = Cl for **2** and **6**, and X = F for **1**. [b] Angle is the dihedral angle between the NiX_2 plane and the NiR_2 plane, where R = C_6F_5 for **2** and **1** and R = $SiCl_3$ for **6**. A dihedral angle of 0° implies a perfect square plane.

halves of the dimeric anion are again related by a crystallographic center of inversion. An ORTEP diagram of the cation is in the supplementary material, and the anion is shown in Figure 2. Fractional coordinates for the asymmetric unit of structure are given in Table IV, and bond distances and angles are listed in Tables V and VI, respectively.

The coordination geometry around the Ni atom is square planar with an average Ni–Si bond length of 2.171 (3) Å. A near-planar local geometry for the Ni coordination sphere is reflected in the rotation angle of only 0.9° between the planes defined by Si(2)–Ni–Si(1) and Ni–Cl(1)–Cl(1′). The Si–Ni–Si bond angle is 89.9 (1)°.

A comparison of relevant bond parameters in **2** and **6** is listed in Table VII. There is a remarkable consistency between the two structures. All of the equivalent parameters are within experimental error. The Ni–Cl bridging length is 2.25 Å, while the Cl–Ni–Cl angle is 86–87° and the Ni–Cl–Ni bridging angle is 93–94°. The distance between Ni atoms in each dimer is 3.28 Å. Thus, the effect of changing the R group from C_6F_5 to $SiCl_3$

Table VIII. Atomic Coordinates in $[(\mu\text{-F})_2Ni_2(C_6F_5)_4][n\text{-}Bu_4N]_2$ (**1**)

atom	*x*	*y*	*z*	*B*,[a] Å^2
Ni	0.45856 (2)	0.54681 (2)	0.45589 (2)	3.85
F(2)	0.4453 (1)	0.50206 (8)	0.5492 (1)	5.28
C(3)	0.4797 (2)	0.5900 (1)	0.3618 (2)	4.62
C(4)	0.4809 (2)	0.5611 (1)	0.2914 (2)	4.62
C(5)	0.4957 (2)	0.5911 (2)	0.2228 (2)	5.26
C(6)	0.5123 (2)	0.6514 (2)	0.2231 (2)	5.14
C(7)	0.5119 (2)	0.6829 (2)	0.2932 (2)	6.07
C(8)	0.4970 (2)	0.6515 (1)	0.3594 (2)	4.97
C(9)	0.3586 (2)	0.5894 (1)	0.4684 (2)	4.63
C(10)	0.2930 (2)	0.5749 (1)	0.4238 (2)	4.66
C(11)	0.2208 (3)	0.6039 (2)	0.4328 (3)	6.82
C(12)	0.2123 (2)	0.6476 (2)	0.4874 (3)	6.80
C(13)	0.2773 (3)	0.6651 (2)	0.5306 (2)	7.28
C(14)	0.3484 (2)	0.6339 (2)	0.5228 (2)	4.81
F(15)	0.4654 (1)	0.49919 (9)	0.2863 (1)	6.52
F(16)	0.4947 (2)	0.5594 (1)	0.1534 (1)	7.25
F(17)	0.5260 (1)	0.6827 (1)	0.1542 (1)	7.96
F(18)	0.5297 (2)	0.7443 (1)	0.2911 (1)	9.02
F(19)	0.4984 (2)	0.68658 (9)	0.4251 (1)	7.07
F(20)	0.2967 (1)	0.5327 (1)	0.3657 (1)	7.18
F(21)	0.1566 (2)	0.5902 (1)	0.3869 (2)	10.70
F(22)	0.1426 (2)	0.6810 (2)	0.4975 (2)	11.77
F(23)	0.2702 (2)	0.7097 (1)	0.5863 (2)	11.17
F(24)	0.4100 (2)	0.6509 (1)	0.5706 (1)	7.59
N(1′)	0.2668 (1)	0.6025 (1)	0.0770 (1)	4.26
C(2′)	0.3429 (2)	0.6311 (2)	0.0411 (2)	5.28
C(3′)	0.3830 (3)	0.5948 (2)	−0.0239 (3)	7.27
C(4′)	0.4525 (3)	0.6356 (3)	−0.0547 (3)	8.85
C(5′)	0.4996 (5)	0.6023 (3)	−0.1156 (5)	14.25
C(6′)	0.2910 (2)	0.5414 (1)	0.1168 (2)	5.63
C(7′)	0.2273 (2)	0.5126 (2)	0.1670 (2)	5.77
C(8′)	0.2605 (3)	0.4506 (2)	0.1992 (3)	8.09
C(9′)	0.1957 (4)	0.4198 (2)	0.2468 (3)	10.27
C(10′)	0.2311 (2)	0.6476 (1)	0.1357 (2)	4.40
C(11′)	0.2867 (2)	0.6653 (2)	0.2015 (2)	5.97
C(12′)	0.2427 (3)	0.7091 (2)	0.2580 (2)	6.73
C(13′)	0.2983 (3)	0.7350 (2)	0.3197 (2)	7.21
C(14′)	0.2041 (2)	0.5860 (1)	0.0143 (2)	5.52
C(15′)	0.1804 (2)	0.6380 (2)	−0.0383 (2)	5.87
C(16′)	0.1139 (3)	0.6158 (2)	−0.0943 (2)	6.66
C(17′)	0.0922 (3)	0.6625 (2)	−0.1551 (3)	8.18
H(2A′)	0.383180	0.636820	0.083360	
H(2B′)	0.327440	0.672290	0.019060	
H(3A′)	0.343980	0.586600	−0.067070	
H(3B′)	0.404430	0.555020	−0.003510	
H(4A′)	0.490250	0.645610	−0.009420	
H(4B′)	0.430750	0.675190	−0.075320	
H(5A′)	0.543940	0.628810	−0.135610	
H(5B′)	0.461620	0.592730	−0.160700	
H(5C′)	0.521120	0.563150	−0.094810	
H(6A′)	0.339620	0.550020	0.150460	
H(6B′)	0.306830	0.511350	0.075260	
H(7A′)	0.177860	0.504470	0.135340	
H(7B′)	0.213630	0.540320	0.211500	
H(8A′)	0.308670	0.458720	0.232620	
H(8B′)	0.276480	0.423400	0.154590	
H(9A′)	0.217190	0.379490	0.267350	
H(9B′)	0.148040	0.411310	0.212950	
H(9C′)	0.180230	0.446630	0.290980	
H(10A′)	0.181840	0.628390	0.158950	
H(10B′)	0.215470	0.685990	0.107120	
H(11A′)	0.335530	0.687110	0.179920	
H(11B′)	0.304990	0.627630	0.230100	
H(12A′)	0.198660	0.685090	0.284910	
H(12B′)	0.218160	0.743450	0.227930	
H(13A′)	0.266670	0.762940	0.354940	
H(13B′)	0.341730	0.759350	0.293600	
H(13C′)	0.322230	0.700990	0.350580	
H(14A′)	0.154600	0.570290	0.040570	
H(14B′)	0.227210	0.552230	−0.019430	
H(15A′)	0.228160	0.652660	−0.069400	
H(15B′)	0.159600	0.673590	−0.006500	
H(16A′)	0.064530	0.605470	−0.063190	
H(16B′)	0.133140	0.577590	−0.121550	
H(17A′)	0.048700	0.646430	−0.189540	
H(17B′)	0.140530	0.673280	−0.186640	
H(17C′)	0.071920	0.701160	−0.128280	

[a] The thermal parameters are of the form $B = 8\pi^2U$.

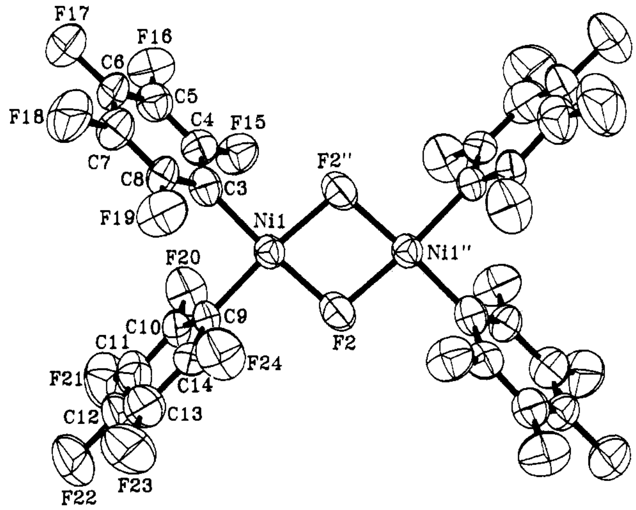

Figure 3. Computer drawing of the $[(\mu\text{-F})_2Ni_2(C_6F_5)_4]^{2-}$ anion as it exists in crystals of the $[n\text{-}Bu_4N^+]_2$ salt.

has no significant affect on the $NiCl_2Ni$ core.

Table IX. Bond Distances (Å) in $[(\mu\text{-F})_2Ni_2(C_6F_5)_4][n\text{-}Bu_4N]_2$ (**1**)

Ni(1)–F(2)	1.886 (2)	C(12)–C(13)	1.363 (6)
Ni(1)–F(2″)	1.919 (2)	C(12)–F(22)	1.377 (5)
Ni(1)–C(3)	1.900 (3)	C(13)–C(14)	1.368 (6)
Ni(1)–C(9)	1.912 (3)	C(13)–F(23)	1.366 (5)
C(3)–C(4)	1.361 (4)	C(14)–F(24)	1.362 (4)
C(3)–C(8)	1.367 (4)	N(1′)–C(2′)	1.538 (4)
C(4)–C(5)	1.368 (5)	N(1′)–C(6′)	1.544 (4)
C(4)–F(15)	1.372 (4)	N(1′)–C(10′)	1.526 (4)
C(5)–C(6)	1.338 (5)	N(1′)–C(14′)	1.539 (4)
C(5)–F(16)	1.376 (4)	C(2′)–C(3′)	1.519 (6)
C(6)–C(7)	1.384 (5)	C(3′)–C(4′)	1.547 (7)
C(6)–F(17)	1.383 (4)	C(4′)–C(5′)	1.493 (9)
C(7)–C(8)	1.348 (5)	C(6′)–C(7′)	1.500 (5)
C(7)–F(18)	1.366 (4)	C(7′)–C(8′)	1.556 (5)
C(8)–F(19)	1.361 (4)	C(8′)–C(9′)	1.507 (8)
C(9)–C(10)	1.368 (4)	C(10′)–C(11′)	1.508 (5)
C(9)–C(14)	1.354 (4)	C(11′)–C(12′)	1.542 (5)
C(10)–C(11)	1.363 (5)	C(12′)–C(13′)	1.513 (6)
C(10)–F(20)	1.356 (4)	C(14′)–C(15′)	1.498 (5)
C(11)–C(12)	1.341 (6)	C(15′)–C(16′)	1.541 (5)
C(11)–F(21)	1.359 (5)	C(16′)–C(17′)	1.499 (6)

Several years ago the observed increase in the X–Ni–X angle from the expected 90° value for a planar $NiBr_2Ni$ bridge was attributed to nonbonded Br- - -Br interactions.[24] Our observed Cl- - -Cl nonbonded interaction is more than 0.40 Å shorter than estimates of a van der Waals contact,[25] yet the Cl–Ni–Cl angle is less than 90°. On this basis, it appears that nonbonded repulsions between bridging halides do not govern deviations from a square geometry. Of course, it should be noted that van der Waals contact distances apply to intermolecular interactions and are normally violated for intramolecular interactions. Typical intramolecular Cl- - -Cl contacts such as those in CCl_4 are 2.9 Å, which are somewhat shorter than those observed in the two dimers. If one uses this 2.9-Å distance as a minimum intramolecular contact distance, then the observed value of 3.08 Å is easily accommodated with a concomitant reduction of the Cl–Ni–Cl angle by some 3–4°.

---

(24) Churchill, M. R.; O'Brien, T. A. *Inorg. Chem.* **1967**, *6*, 1386.

(25) Bondi, A. *J. Phys. Chem.* **1964**, *68*, 441.

Table X. Bond Angles (deg) in $[(\mu\text{-F})_2Ni_2(C_6F_5)_4][n\text{-}Bu_4N]_2$ (**1**)

F(2)–Ni(1)–F(2″)	81.41 (7)	C(9)–C(10)–C(11)	122.04 (32)
F(2)–Ni(1)–C(3)	175.91 (11)	C(9)–C(10)–F(20)	122.08 (28)
F(2)–Ni(1)–C(9)	93.02 (11)	C(11)–C(10)–F(20)	115.83 (30)
F(2″)–Ni(1)–C(3)	94.63 (11)	C(10)–C(11)–C(12)	119.92 (38)
F(2″)–Ni(1)–C(9)	174.11 (11)	C(10)–C(11)–F(21)	121.51 (36)
C(3)–Ni(1)–C(9)	90.97 (13)	C(12)–C(11)–F(21)	118.56 (37)
Ni(1)–F(2)–Ni(1″)	98.59 (8)	C(11)–C(12)–C(13)	119.60 (39)
Ni(1)–C(3)–C(4)	121.94 (23)	C(11)–C(12)–F(22)	123.32 (39)
Ni(1)–C(3)–C(8)	123.15 (25)	C(13)–C(12)–F(22)	116.74 (37)
C(4)–C(3)–C(8)	114.88 (30)	C(12)–C(13)–C(14)	119.46 (35)
C(3)–C(4)–C(5)	123.14 (29)	C(12)–C(13)–F(23)	120.66 (42)
C(3)–C(4)–F(15)	120.44 (27)	C(14)–C(13)–F(23)	119.63 (40)
C(5)–C(4)–F(15)	116.41 (27)	C(9)–C(14)–C(13)	121.94 (33)
C(4)–C(5)–C(6)	119.99 (32)	C(9)–C(14)–F(24)	120.97 (30)
C(4)–C(5)–F(16)	120.30 (28)	C(13)–C(14)–F(24)	117.05 (30)
C(6)–C(5)–F(16)	119.71 (30)	C(2′)–N(1′)–C(6′)	108.14 (24)
C(5)–C(6)–C(7)	119.09 (32)	C(2′)–N(1′)–C(10′)	108.83 (22)
C(5)–C(6)–F(17)	120.78 (31)	C(2′)–N(1′)–C(14′)	111.69 (23)
C(7)–C(6)–F(17)	120.07 (29)	C(6′)–N(1′)–C(10′)	111.17 (23)
C(6)–C(7)–C(8)	118.90 (30)	C(6′)–N(1′)–C(14′)	106.66 (22)
C(6)–C(7)–F(18)	117.29 (31)	C(10′)–N(1′)–C(14′)	110.34 (22)
C(8)–C(7)–F(18)	123.76 (32)	N(1′)–C(2′)–C(3′)	116.34 (29)
C(3)–C(8)–C(7)	123.95 (32)	C(2′)–C(3′)–C(4′)	106.23 (37)
C(3)–C(8)–F(19)	121.72 (29)	C(3′)–C(4′)–C(5′)	110.60 (51)
C(7)–C(8)–F(19)	114.32 (26)	N(1′)–C(6′)–C(7′)	115.36 (28)
Ni(1)–C(9)–C(10)	121.12 (23)	C(6′)–C(7′)–C(8′)	108.35 (33)
Ni(1)–C(9)–C(14)	122.08 (25)	C(7′)–C(8′)–C(9′)	108.88 (42)
C(10)–C(9)–C(14)	116.77 (30)	N(1′)–C(10′)–C(11′)	114.85 (25)
C(10′)–C(11′)–C(12′)	109.75 (29)	C(14′)–C(15′)–C(16′)	109.14 (29)
C(11′)–C(12′)–C(13′)	112.35 (34)	C(15′)–C(16′)–C(17′)	113.23 (32)
N(1′)–C(14′)–C(15′)	115.11 (26)		

Next the structure of **1** will be compared with that of **2** so that the effect of the μ-F bridge can be assessed, relative to that of the μ-Cl bridge. The X-ray structure of **1** contains half of an anion and one cation in the asymmetric unit of structure. An ORTEP diagram of the anion of **1** is shown in Figure 3. Tables of fractional coordinates, bond distances, and bond angles are listed in Tables VIII–X, respectively.

The structure of the anion in **1** is similar to that in **2**. A square-planar geometry is observed as in **2** and as predicted by Summerville and Hoffmann[26] for a halide bridge. The rotation angle between the planes defined by NiC_3C_9 and NiF_2F_2'' is 2.2°. The two C_6F_5 groups are rotated 23.6 and 16.4° from the normal to the coordination plane, which apparently results from differences in the packing between **1** and **2**. It is interesting to note that **1** is the first totally fluorinated organotransition-metal complex and the first structurally characterized nickel complex containing a fluoride bridge.

The substitution of a fluoride for chloride in the $[R_2NiX_2NiR_2]^{2-}$ core represents a large change considering the much smaller size and reduced polarizability of fluoride. Indeed, the Ni–F distance of 1.903 (2) Å is reduced by 0.35 Å from the Ni–Cl distance in **2** (Table VII). Consideration of normal van der Waals contacts[25] indicates that the F- - -F nonbonded distance should be more than 0.5 Å smaller than that of chloride. The observed F- - -F contact in **1** is 0.60 Å smaller than the chloride contact in **2**, and the Ni- - -Ni distance is reduced by 0.4 Å. Moreover, the F–Ni–F angle is reduced by 5° as the halide bridges move closer together. Although the change is much more subtle, there is also a slight increase in the arene Ni–C_6F_5 distance by 0.026 Å. This suggests that there is a slightly less π-back-bonding (Ni→C_6F_5) in the fluoride dimers, which could be the effect of poorer π-donation by fluoride verses chloride. If one accepts bond-angle deformation arguments presented by Domenicano and co-workers,[27] then further support for this effect is provided by the larger internal ring angle at the σ-bonded carbon of the C_6F_5 group, which has an average value of 116° in **1** and 113° in **2**. This internal ring angle is expected to decrease as the nickel atom becomes more σ-electron releasing or more π-bonding.[27,28] It follows that the chloride being less electronegative and a better π-donor produces a nickel atom that is a better σ-donor and a better π-donor to the C_6F_5 group than fluoride.

Experimental Section

All manipulations were carried out under anaerobic conditions by using standard Schlenkware and a Vacuum Atmospheres drybox. Nitrogen gas was dried by passing over a heated column containing molecular sieves and catalyst R3-11 by Chemical Dynamics Corp.

Solvents employed were reagent grade and refluxed under a nitrogen atmosphere and appropriate drying agents. The following is a list of the solvents with drying agents in parentheses: pentane, heptane, toluene, dichloromethane (CaH_2); diethyl ether, tetrahydrofuran (sodium benzophenone ketyl); acetonitrile (P_4O_{10}).

Reagents used are all commerically available. Elemental analysis was performed by Schwarzkopf Micro Lab, 56-19 37th Avenue, Woodside, NY, and Galbraith Laboratories, Knoxville, Tennessee.

Preparation and Characterization of $[Et_4N]_2[(\mu\text{-Cl})Ni(C_6F_5)_2]_2 \cdot CH_2Cl_2$ (2). To a stirring solution of (η^6-toluene)$Ni(C_6F_5)_2$ (0.05 g, 0.10 mmol) at room temperature under N_2 in CH_2Cl_2 (10 mL) were added crystals of Et_4NCl (0.017 g, 0.10 mmol). Immediately the red-brown solution turned orange-red. The solution was filtered and dried in vacuo to a crystalline solid. The solid was redissolved in an excess of CH_2Cl_2 (5 mL) and toluene (5 mL) layered on top of the solution. This mixture was left open to the drybox atmosphere for 4 days and resulted in a good crop of crystals. The crystals were washed with pentane and dried. X-ray analysis revealed a CH_2Cl_2 solvate. For analysis, the CH_2Cl_2 solution was diluted with pentane to yield the unsolvated dimer. Yield: 0.471 g, 0.42 mmol, 84%.

^1H NMR (400 MHz, CD_2Cl_2, CH_2Cl_2 reference) $\delta(CH_2)$ 3.51 (mult), δ (CH_3) 1.40 (mult in 2:3 ratio).

IR (Nujol/KBr; Nujol/polyethylene): 1670 (vw), 1660 (vw), 1500 (vs), 1470 (vs), 1385 (s), 1350 (w), 1282 (w), 1255 (vw), 1178 (s), 1055 (s), 1010 (m), 960 (vs), 785 (s), 750 (s), 703 (vw), 338 (m), 313 (m), 240 cm^{-1} (vw).

Anal. Calcd for $C_{40}H_{40}F_{20}N_2Cl_2Ni_2$: C, 43.01; H, 3.61; N, 2.50. Found: C, 42.24; H, 3.50; N, 2.44.

Red-orange crystals were obtained from CH_2Cl_2 and mounted on a glass fiber with epoxy glue. The crystal habit was triclinic, and 15 reflections $2\theta > 25°$ were used in the least-squares refinement of the unit cell. Data collection was on a Syntex P2$_1$ graphite monochromated CuKα' radiation in θ–2θ scan mode. Scan range was 1.3° below Kα' and 1.3° above Kα'. Scan speed was variable at 1.5–20°/min. Two check reflections were monitored every 100 measurements. The agreement factor $R_s = 0.021$ ($R_s = \sum|I_o - \langle I_o\rangle|/\sum|I_o|$. A decay correction was applied for changes in check reflection intensity with the maximum correction for I_0 being 1.285. The absorption correction was empirical. The structural problem was solved by using Patterson and Fourier methods. Major programs used were FBLX, FFT, and PEAK. The $[Et_4N]^+$ cations were located on crystallographic centers of inversions. A model incorporating an ordered nitrogen with disordered ethyl groups conforming to i symmetry was utilized. Rigid-body refinement was employed for the cation using a C–N distance of 1.52 Å, a C–C distance of 1.54 Å, and bond angles of 109.5°. Hydrogen atom positions were not located. Anomalous dispersion corrections were applied for Ni and Cl. Block-diagonal least-squares calculations (one for the anion, the other for the cation) were used. All calculations were performed on a Honeywell 66/6000 computer at the University of Kansas. Because block-diagonal refinement was used, some of the errors in bond parameters are underestimated. (The body-centered unit cell selected for the structure determination corresponds to a reduced cell of $P\bar{1}$ symmetry with lattice constants $a = 11.986$ Å, $b = 12.761$ Å, $c = 10.618$ Å, $\alpha = 113.45°$, $\beta = 113.71°$, and $\gamma = 94.25°$; see Table XI.)

Preparation and Characterization of $[n\text{-}Bu_4N]_2[(\mu\text{-F})Ni(C_6F_5)_2]_2$ (1). To a stirred solution of (η^6-toluene)$Ni(C_6F_5)_2$ (0.5 g, 1.03 mmol) in CH_2Cl_2 (30 mL) was added a THF solution of n-Bu_4NF (1 M THF, 1.0 mL, 1.00 mmol) dropwise. A subtle color change occurred (red-brown to orange brown). Solvent was quickly removed, as the ammonium fluoride solution contained up to 5% water. The dry residue was redissolved in CH_2Cl_2 and the solution filtered. A considerable amount of metallic residue was deposited on the filter frit. The solution was again pumped to dryness and the resultant solid washed three times with pentane (20 mL) and redissolved in CH_2Cl_2, and then n-heptane was layered onto the orange solution. Within 4 days, large orange plates had precipitated. The supernatant was removed and discarded. The product,

---

(26) Summerville, R. H.; Hoffman, R. *J. Am. Chem. Soc.* **1976**, *98*, 7240.

(27) Domenicano, A.; Vaciago, A.; Coulson, C. A. *Acta Crystallogr., Sect. B* **1975**, *B31*, 221. Domenicano, A.; Vaciago, A. *Acta Crystallogr., Sect. B* **1979**, *B35*, 1382.

(28) Eyring, M. W.; Zuerner, E. C.; Radonovich, L. J. *Inorg. Chem.* **1981**, *20*, 3405.

Table XI. Crystal Data for $[(\mu\text{-Cl})_2Ni_2(C_6F_5)_4][(C_2H_5)_4N]_2\cdot CH_2Cl_2$ (**2**), $[(\mu\text{-F})_2Ni_2(C_6F_5)_4][(C_4H_9)_4N]_2$ (**1**),[a] and $[(\mu\text{-Cl})_2Ni_2(SiCl_3)_4][((CH_3)_3C)_2C_5H_3NH]_2$ (**6**)

	2	**1**	**6**
formula	$C_{41}H_{42}F_{20}N_2Cl_4Ni_2$	$C_{56}H_{72}F_{22}N_2Ni_2$	$C_{26}H_{44}Cl_{14}N_2Si_4Ni_2$
fw	1201.96	1308.56	2221.42
space group	$I\bar{1}$ (No. 2)	*Pbca* (No. 61)	$P2_1/n$ (No. 14)
a, Å	10.618 (2)	16.601 (3)	11.686 (2)
b, Å	13.652 (3)	21.717 (5)	11.683 (2)
c, Å	18.144 (3)	17.158 (4)	17.272 (4)
α, deg	86.20 (2)	90	90
β, deg	89.18 (2)	90	87.645 (6)
γ, deg	93.02 (2)	90	90
Z	2	4	2
V, Å^3	2620.25	6185.87	2355.95
ρ, g/cm^3	1.523	1.405	1.57
temp, °C	25 ± 2	25 ± 2	24
radiation (λ, Å)	Cu Kα (1.5418)	Mo Kα (0.71069)	Mo Kα (0.71069)
R^b	0.0536	0.0664	0.054
$R_w{}^c$	0.0605	0.0684	0.067
μ, cm^{-1}		7.19	17.3

[a] This *I*-centered cell corresponds to a reduced cell of $P\bar{1}$ symmetry with the following lattice constants: $a = 11.9865$ Å, $b = 12.7612$ Å, $c = 10.6180$ Å, $\alpha = 113.45°$, $\beta = 113.71°$, $\gamma = 94.25°$. [b] $R = \sum||F_o| - K|F_c||/\sum|F_o|$. [c] $R_w = [\sum w(|F_o| - K|F_c|)^2/\sum w|F_o|^2]^{1/2}$.

an air-stable orange crystalline solid, was isolated (0.340 g, 0.26 mmol, 61%). Mp: discolored at 150 °C.

^{1}H NMR (400 MHz, CD_2Cl_2, CH_2Cl_2 reference): $\delta(CH_3)$ 0.98, $\delta(CH_2)$ 1.42, 1.70, 3.33 (broad and unresolved).

IR (Nujol/KBr; Nujol/polyethylene): 1635 (vw), 1605 (vw), 1500 (vs), 1460 (vs), 1380 (s), 1283 (w), 1255 (vw), 1175 (w), 1115 (vw), 1100 (vw), 1050 (s), 1040 (sh), 950 (vs), 890 (w), 875 (w), 810 (vw), 775 (s), 735 (m), 720 (sh), 520 (m), 445 (m), 348 (m), 240 (w), 220 cm^{-1} (w).

A red-brown crystal of **1** was mounted as for **2**. The crystal habit was orthorhombic. The linear absorption coefficient was 7.191 cm^{-1}. Intensity collection was as in **2** by using Mo Kα radiation. $R_s = 0.031$ with maximum decay correction of 1.143. The structure was solved by using the heavy-atom method. Hydrogen atom positions were located, but the methyl hydrogens were not resolved in the difference map. Idealized hydrogen positions were calculated and added into the structure factor calculations but were not refined. The cation was treated as a rigid body with idealized parameters of 1.52 Å for the C–N lengths, 1.54 Å for the C–C lengths, and 109.5° for the bond angles. Block-diagonal least squares (scale and thermal parameters in one block and positional parameters in another) was used for refinement. Because block-diagonal refinement was used, some of the errors in bond parameters are underestimated.

Preparation and Characterization of $[2,6\text{-}t\text{-}Bu_2py]_2[(\mu\text{-Cl})Ni(SiCl_3)_2]_2$ (6). To a solution of 2 g (10 mmol) of 2,6-di-*tert*-butylpyridine (used as received, slightly wet) in 50 mL of CH_2Cl_2 was added 0.5 g (0.9 mmol) of (η^6-toluene)$Ni(SiCl_3)_2$, and the resulting solution was stirred for 2–3 h, after which the color changed from red to a distinct brown red. The solution was filtered and thoroughly layered with 80 mL of pentane and kept at 0 °C (ice bath) for 1 week. After that time the now orange solution was carefully decanted and the small deep red needlelike and rectangular-shaped crystals were dried under vacuum. The yield was >80%. The material is best stored in a refrigerator; otherwise decomposition occurs in a few days.

IR (Nujol mull): 3360 (m), 1605 (s), 1525 (m), 1245 (m), 1185 (m), 1145 (w), 880 (w), 840 (s), 780 (s), 540 (vs), 505 (vs), 475 cm^{-1} (vs).

IR (Fluorolube, CsI): 3360 (m), 2960 (m), 2920 (sh), 2820 (sh), 1605 (s), 1525 (m), 1460 (w, b), 1360 cm^{-1} (w).

MS (133 °C, 29eV, EI) [*m/e* (relative intensity) assignment]: 325.9 (9.28) $C_{13}H_{21}NSiCl_3{}^+$, 290 (2.38) $C_{13}H_{21}NSiCl_2{}^+$, 268 (1.04) $Si_2Cl_6{}^+$, 254 (0.34) $C_{13}H_{21}NSiCl^+$, 191 (100.0) $C_{13}H_{21}N^+$.

^{13}C NMR (CD_2Cl_2; δ ppm): 30.40, 37.92, 115.82, 124.10, 136.60.

Anal. Calcd for $C_{13}H_{21}NClNiSi_2$ (504.4): C, 30.92; H, 4.16; N, 2.78; Ni, 11.70.

Found: C, 30.42; H, 4.41; N, 2.37; Ni, 11.82.

Table XII. Yields and Properties of **3–5**[a]

	% yield	mp, °C	anal.		
			atom	% found	% calcd
$[n\text{-}Bu_4N]_2[(\mu\text{-F})Ni(SiCl_3)_2]_2$ (**3**)	40	130–150	C	31.50	32.60
			H	6.30	6.16
$[n\text{-}Bu_4N]_2[(\mu\text{-Cl})Ni(SiCl_3)_2]_2$ (**4**)	61	120–140			
$[n\text{-}Bu_4N]_2[(\mu\text{-Br})Ni(SiCl_3)_2]_2$ (**5**)	58	145–160	C	31.00	29.56
			H	6.09	5.58

[a] All compounds exhibited very similar IR spectra (Nujol/KBr): medium to strong bands were found at 470 (s), 540 (s), 740 (s), 800 (m), 1035 (s), 1060–1110 (s, br), and 1170 cm^{-1} (s).

Rectangular crystals of the compound were wedged inside 0.30-mm thin-walled glass capillaries with brief exposure to air. A summary of the crystal data is given in Table XI. The intensity of three standard reflections monitored after every 97 data points decreased by 11% over the course of data collection. A decay correction was applied to the data. The structure was determined by using Patterson and Fourier techniques.[29] Full-matrix isotropic refinement produced an *R* value of 13%. This was followed by fully anisotropic refinement, which converged with an *R* value of 5.4%. A difference map at this stage of refinement clearly revealed positions of electron densitites for the hydrogen atoms on N(1), C(3), and C(4) as well as several of the methyl hydrogen atoms. Theoretical positions for the four aromatic hydrogens were then calculated and included as fixed contributors in the final cycles of refinement, which converged with an *R* value of 5.4% and an R_w value of 6.7%. No absorption corrections were applied to the data. Absorption factors were estimated to range from 0.70 to 0.88 for the irregularly shaped crystal.

The analogues **3–5** of structure **6** have been prepared with $n\text{-}Bu_4N^+$ as cation.[30]

General Procedure for Preparing 3–5. A 0.610-g portion (1.45 mmol) of (η^6-toluene)$Ni(SiCl_3)_2$ dissolved in 30 mL of toluene was added into a 200-mL Schenk tube through a fine glass filter frit. To the red-brown solution was added dropwise 1 mmol of $(n\text{-}Bu)_4NX$ in 5 mL of CH_2Cl_2 over a 5-min period. The mixture was stirred for 10 min and filtered. The solid collected was washed with 20 mL of toluene and then dissolved in 20 mL of CH_2Cl_2. The solution was filtered through a fine frit and solvent removed under vacuum. Yields and properties are collected in Table XII.

Acknowledgment. The support of the National Science Foundation is acknowledged with gratitude. J.S. thanks the Fulbright Commission for a travel grant and the Verband der Chemischen Industrie for financial support. We also thank Dr. F. Takusagawa for diffraction analysis of **1** and **2** and S. B. Choe for experimental assistance.

Supplementary Material Available: An ORTEP diagram of the $[((CH_3)_3C)_2(C_5H_3NH)]^+$ cation (Figure IV), crystal data for **1**, **2**, and **6** (Table XI-S), anisotropic thermal parameters for **2** (Table XIII), thermal parameters for **6** and **1** (Tables XV and XVII), and least-squares planes data for **6** (Table XIX) (9 pages); structure factors for **1**, **2**, and **6** (Tables XVIII, XIV, and XVI) (49 pages). Ordering information is given on any current masthead page.

---

(29) The programs used in this structure determination were supplied by Crystal Logic. The Crystal Logic package includes modified versions of the following programs: REDUCE (Broach, Coppens, Becker, and Blessing), peak profile analysis, Lorentz and polarization corrections; MULTAN (Main, Germain, and Woolfson), package of programs, including direct methods, structure factor normalization, Fourier transform, and peak search; ORFLS (Busing, Martin and Levy), structure factor calculation and full-matrix least-squares refinement; ORFFE (Busing, Martin, and Levy), distance, angle, and error calculations; ABSROB (Coppens, Edwards, and Hamilton), absorption correction calculation; ORTEP (Johnson) figure plotting; HYDROGEN (Trueblood), calculation of hydrogen atomic positions. All calculations were performed on a DEC MicroVax II computer. Scattering factors and corrections for anomalous dispersion were taken from: *International Tables for X-ray Crystallography*; Kynoch Press: Birmingham, England, 1974; Vol. IV.

(30) Choe, S. B. Ph.D. Thesis, Kansas State University, 1987.